Journal of Pest Science (2024) 97:411–427
https://doi.org/10.1007/s10340-023-01623-7

ORIGINAL PAPER

In planta RNAi targeting *Meloidogyne incognita Minc16803* gene perturbs nematode parasitism and reduces plant susceptibility

Valdeir Junio Vaz Moreira[1,2,3] · Daniele Heloísa Pinheiro[1,4] · Isabela Tristan Lourenço-Tessutti[1,4] · Marcos Fernando Basso[1,4] · Maria E. Lisei-de-Sa[1,4,5] · Maria C. M. Silva[1,4] · Etienne G. J. Danchin[4,7] · Patrícia M. Guimarães[1,4] · Priscila Grynberg[1,4] · Ana C. M. Brasileiro[1,4] · Leonardo L. P. Macedo[1,4] · Carolina V. Morgante[1,4,6] · Janice de Almeida Engler[6,4] · Maria Fatima Grossi-de-Sa[1,4,8]

Received: 1 November 2022 / Revised: 22 February 2023 / Accepted: 13 April 2023 / Published online: 13 May 2023

Abstract

Meloidogyne incognita is one of the most important plant-parasitic nematodes (PPNs) causing severe crop losses worldwide. Plants have evolved complex defense mechanisms to respond to PPNs attacks. Conversely, PPNs have evolved infection mechanisms that involve the secretion of effector proteins into host plants to suppress immune responses and facilitate parasitism. Therefore, effector genes are attractive targets for the genetic improvement of plant resistance to *M. incognita*. In this study, we functionally characterized the *Minc16803* (*Minc3s00746g16803*) putative effector gene to evaluate its role during plant-nematode interactions. First, we found that the *Minc16803* gene is expressed in all nematode life stages and encodes a protein with an N-terminal signal peptide for secretion, a motif characteristic of effector proteins and with the absence of transmembrane domain. In addition, our data demonstrated that transgenic *Arabidopsis thaliana* lines overexpressing a *Minc16803*-dsRNA efficiently downregulated the *Minc16803* transcripts in infecting nematodes. Furthermore, transgenic lines were significantly less susceptible to *M. incognita* compared to wild-type control plants. The number of galls per plant was reduced by up to 84%, while the number of egg masses per plant decreased by up to 93.3%. Moreover, galls and feeding sites in the roots of transgenic lines were smaller than those in the control plants. Histological analysis revealed giant cells without cytoplasm, disordered neighboring cells, and malformed maturing nematodes in transgenic galls. Curiously, numerous hatching ppJ2 juveniles were often observed near the female body within the transgenic root tissues before egg mass extrusion. All findings strongly suggest that *Minc16803* gene is a promising target to engineer agricultural crops for *M. incognita* resistance through host-induced gene silencing.

Keywords Host-induced gene silencing · dsRNA · Plant-nematode interactions · Root-knot nematode

Communicated by Aurelio Ciancio.

Valdeir Junio Vaz Moreira, Daniele Heloísa Pinheiro have contributed equally to this work.

✉ Maria Fatima Grossi-de-Sa
fatima.grossi@embrapa.br

[1] Embrapa Genetic Resources and Biotechnology (Cenargen), PqEB Final, W5 Norte, PO Box 02372, Brasília, DF, Brazil

[2] Biotechnology Center, PPGBCM, UFRGS, Porto Alegre, RS, Brazil

[3] Federal University of Brasília, UNB, Brasília, DF, Brazil

[4] National Institute of Science and Technology, INCT PlantStress Biotech, Embrapa-Brazil, Brasília, DF, Brazil

[5] Agricultural Research Agency of Minas Gerais (EPAMIG), Uberaba, MG, Brazil

[6] Embrapa Semiarid, Petrolina, PE, Brazil

[7] INRAE, CNRS, Université Côte d'Azur, ISA, Sophia-Antipolis, Nice, France

[8] Catholic University of Brasília, Brasília, DF, Brazil

Introduction

The co-evolutionary interactions between pathogens and their host plants have driven the development of complex mechanisms of pathogen infection and plant immune defense (Zhang et al. 2020). Plant-parasitic nematodes (PPNs) have evolved a striking diversity of mechanisms to overcome plant defenses. One of the mechanisms used by PPNs for successful infection involves the secretion of several effector proteins produced by esophageal glands into plant root cells through their stylet (Jagdale et al. 2021). Nematode effectors generally impair plant immune responses by interfering with different host metabolic and physiological processes, such as hormone-dependent defense pathways (Habash et al. 2017), secondary metabolite pathways (Bauters et al. 2020), actin filaments organization (Leelarasamee et al. 2018), cell cycle onset and progression (Coke et al. 2021), protein ubiquitination, and gene expression regulation (Diaz-Granados et al. 2020).

The root-knot nematode (RKN) *Meloidogyne incognita* attacks a wide range of agronomically important crops and seriously threatens crop production worldwide (Bernard et al. 2017). The *M. incognita* life cycle includes six stages, egg, ppJ2 (pre-parasitic second-stage juveniles), pJ2 (parasitic second-stage juveniles), J3, J4 non-feeding juveniles, and adult females (Triantaphyllou and Hirschmann 1960; Castagnone-Sereno et al. 2013). The *M. incognita* pJ2s secrete several effector proteins that trigger the differentiation of root vascular parenchymal cells into 5–7 specialized, multinucleate, and hypertrophied feeding cells, named giant cells, which are formed by successive nuclear divisions without cytokinesis (Kyndt et al. 2013). The galls formed in host roots are the typical symptoms of *M. incognita* infection and result from the proliferation of the tissue around the nematode and giant cells. The feeding cells exhibit high metabolic activity and provide all nutrients required for nematodes to complete their life cycle (Siddique and Grundler 2018). Studies have revealed that *M. incognita* secretes an arsenal of effector proteins into host plant root cells that can interact with different target proteins of parasitized plants. The interaction between nematode effectors and targeted plant proteins triggers molecular, physiological, and morphological changes that culminate in the formation of permanent feeding sites (Jagdale et al. 2021). For instance, the *M. incognita* MIF-like effector facilitates nematode parasitism by interacting with plant Annexin 1 and Annexin 4, and subsequently suppressing host signal transduction and immune responses (Zhao et al. 2019). The *M. incognita* Mi-ISC-1 effector suppresses plant salicylic acid biosynthesis (Qin et al. 2021), and Mj2G02 effector from *Meloidogyne javanica* impairs cell death by disrupting jasmonic acid-mediated signaling to promote parasitism (Song et al. 2021). Similarly, the *M. incognita* effector MiEFF1 targets *A. thaliana* cytosolic glyceraldehyde-3-phosphate dehydrogenases and universal stress proteins, which are involved in the regulation of salicylic acid and jasmonic defense-related genes expression (Truong et al. 2021). Mendes et al. (2021a) showed that the Minc00344 and Mj-NULG1a effector proteins interact with GmHub10 soybean protein to promote *M. incognita* and *M. javanica* parasitism, respectively. Mendes et al. 2021b also reported that MiEFF1/Minc17998 effector protein interacts with GmHub6 protein to promote *M. incognita* parasitism in soybean plants.

Host-induced gene silencing (HIGS) provides a promising strategy toward increased plant resistance to nematodes (Basso et al. 2020; Lisei-de-Sá et al. 2021). A number of studies have demonstrated that transgenic plants expressing engineered dsRNAs can efficiently trigger the silencing of essential genes or parasitism genes of nematodes (Huang et al. 2006; Sindhu et al. 2009; Souza Júnior et al. 2013; Lourenço-Tessutti et al. 2015). Since effectors can contribute substantially to nematode pathogenicity, their silencing is expected to impair nematode infection. Therefore, effector genes are attractive targets for developing RNAi-based transgenic plants with reduced susceptibility to PPNs. Previous functional studies using RNAi-plants have provided experimental evidence that diverse nematode effectors, such as *Heterodera schachtii* 30D08 and Hs25A01 (Pogorelko et al. 2016; Verma et al. 2018), *Heterodera glycines* Hg16B09 (Hu et al. 2019), *Meloidogyne graminicola* Mg01965 (Zhuo et al. 2019) and MgMO237 (Chen et al. 2018), and *Meloidogyne enterolobii* MeTCTP (Zhuo et al. 2017) contribute significantly to nematodes parasitism. With respect to *M. incognita* effectors, it was demonstrated that transgenic *A. thaliana* plants that expressed a dsRNA targeting *MiMsp40* were less susceptible to *M. incognita*, as evidenced by decreased number of galls and eggs (Niu et al. 2016). Moreira et al. 2022 showed that downregulation of the *Minc03328* effector gene triggered by *in planta* RNAi strategy decreased the number of galls (85%), egg masses (90%), and the ratio [number of egg masses/number of galls] (87%) and consequently reduced the plant susceptibility to *M. incognita.*

The identification and characterization of the effectors employed by *M. incognita* to counteract plant defense responses and the mechanistic basis of effector activity in plants provide important insights into the biology of plant-nematode interactions (Vieira and Gleason 2019). In addition, this knowledge can be helpful in developing more effective control methods against *M. incognita*. An increasing number of putative nematode effectors have been described, but detailed information on the functional role of effectors involved in *M. incognita* parasitism is still lacking (Bellafiore et al. 2008; Gardner et al. 2018; Grynberg et al. 2020).

Here, we identified and functionally characterized a putative effector, named Minc16803. We found that *Minc16803* gene is transcriptionally expressed in all nematode stages, including pJ2, J3, J3/J4, adult females, and eggs. This gene encodes a protein with a predicted secretory N-terminal signal peptide and a motif characteristic of known effectors, reinforcing its potential as an effector protein. Furthermore, we demonstrated that transgenic *A. thaliana* lines overexpressing a dsRNA targeting the *Minc16803* transcripts significantly suppressed plant infection by *M. incognita*. Morphological analyses of *M. incognita*-induced galls in transgenic roots strongly suggest that the Minc16803 protein might contribute to the proper development of feeding sites in the host plant. Curiously, these analyses also revealed malformed maturing nematodes and ppJ2s near the female body, which hatched from eggs prior egg mass extrusion on root surface. Taken together, all data indicate that the putative effector protein Minc16803 plays a key role in *M. incognita* parasitism and may be a valuable target for plant-mediated RNAi control of nematodes.

Material and methods

Minc16803 gene sequence

The putative *Minc16803* effector gene was identified based on comparative genomic and transcriptomic analysis. Briefly, we searched for proteins having a predicted signal peptide for secretion, no transmembrane region, and harboring protein motifs characteristic of effector at the N-terminal region. In addition, we required the protein to be encoded by a gene expressed at all developmental stages of the *M. incognita* life cycles and being in maximum 3 copies, consistent with the triploid genome structure. The *Minc16803* (*Minc3s00746g16803*) sequence and its two paralogous *Minc3s00070g03473* and *Minc3s00200g07395* genes (Suppl. File S1) were retrieved from the BioProject ID PRJEB8714 (sample: ERS1696677) (Blanc-Mathieu et al. 2017) in the WormBase Parasite Database version WBPS16 (Lee et al. 2018). Subsequently, conserved domains in the *Minc16803* gene sequence were identified using CDD Database from NCBI (Marchler-Bauer et al. 2015), PFAM Database from EMBL-EBI (El-Gebali et al. 2019), and InterPro Scan (Blum et al. 2021), while the nuclear localization signal was predicted with a cutoff value of 0.5 using the NLStradamus online tool (Nguyen Ba et al. 2009). Secretory signal peptides were predicted using the MatureP tool (Orfanoudaki et al. 2017) and SignalP 5.0 program (Almagro Armenteros et al. 2019), whereas putative transmembrane domains were predicted using the TMHMM program (Möller et al. 2001). In addition, we used the MERCI software (Vens et al. 2011) to check whether protein motifs enriched at the N-terminal region of known effector proteins could be identified in *Minc16803*.

In silico expression level of the *Minc16803* gene

The expression levels of the *Minc16803* gene and its two paralogous genes *Minc3s00200g07395* and *Minc3s00070g03473* at different *M. incognita* life stages were retrieved from WormBase Parasite (Howe et al. 2017), in the 'Expression' section, sub-section 'Life Cycle' of gene-based displays. In short, in WormBase Parasite, RNA-seq data of five *M. incognita* developmental life stages (egg, J2, pJ2/J3, J4, and female), generated in triplicates (Choi et al. 2017), were aligned on the *M. incognita* annotated genome (Blanc-Mathieu et al. 2017) using TopHat2 (Kim et al. 2013). Expression values in Transcripts Per Million units (TPM) were determined from the aligned reads using HTSeq (Anders et al. 2015).

Meloidogyne incognita race 3 inoculum

Meloidogyne incognita race 3 inoculum was maintained on tomato plants (*Solanum lycopersicum* cv. Santa Cruz) under greenhouse conditions. Infected roots were collected at 90 days after infection (DAI), rinsed with water, and then grounded for 30 s in a 0.5% sodium hypochlorite solution using a blender. The suspension was sieved through a set of sieves (45, 100, and 500-mesh), while eggs were collected on the 500-mesh sieve. The collected eggs were submitted to the Baermann funnel technique, and hatched ppJ2s were transferred to a Becker with sterile distilled water and sequentially decanted at 4 °C for 7–14 days. For gene expression assays, eggs were collected as previously described, re-suspended in an inert suspension of kaolin substrate, and centrifuged at 2,500 rpm for 5 min. The precipitated material was re-suspended in a 30% (w/v) sucrose solution and centrifuged again at 2,500 rpm for 5 min. Finally, the supernatant was passed through a 500-mesh sieve, and the eggs retained on the sieve were rinsed in sterile water and immediately frozen in liquid nitrogen.

Meloidogyne incognita development in wild-type *Nicotiana tabacum* roots

The *N. tabacum* var. Petit Havana (SR1) plants were inoculated with 1,000 ppJ2s of *M. incognita* and maintained under greenhouse conditions. Infected roots were harvested during nematode parasitism at 5, 10, 15, and 22 DAI, washed with water, dried with paper towels, and stained with acid fuchsin according to Bybd et al. 1983. Then, root samples were immersed in 2.5% (v/v) sodium hypochlorite solution for clarification and washed with water for 10 min. Finally, the clarified roots were completely immersed in acid fuchsin

solution (1.25 g acid fuchsin solubilized in 1:3 v/v glacial acetic acid and distilled water). For better root staining, samples were slightly heated in a microwave for 1 min. After the staining step, the acid fuchsin solution was discarded; roots were rinsed and transferred to acidified glycerol solution (24:1 v/v glycerol and hydrochloric acid). Nematode stages were then visualized in galls under a stereomicroscope and imaged using a Zeiss Axiocam MR.

Minc16803 expression level during *M. incognita* parasitism in wild-type *N. tabacum*

Total RNA was extracted from *M. incognita* eggs, ppJ2, and infected *N. tabacum* galls at 5, 10, 15, and 22 DAI, using Quick-RNA™ Plant Mini-prep kit (Zymo Research, Irvine, CA, USA). RNA concentration was determined using a spectrophotometer (NanoDrop 2000, Thermo Scientific, Massachusetts, USA), and integrity was assessed in 1% agarose gel electrophoresis. RNA samples were treated with RNase-free RQ1 DNase I (Promega, Madison, Wisconsin, USA) according to the manufacturer's instructions. DNase-treated RNA was used as a template for cDNA synthesis using oligo-$(dT)_{20}$ primer (100 µM), random hexamers (50 µM), and SuperScript III RT (Life Technologies, Carlsbad, CA, USA) according to the manufacturer's instructions. RT-qPCR assays were performed in an Applied Biosystems 7500 Fast Real-Time PCR System (Applied Biosystems, Foster City, CA, USA) using 2 µl cDNA (diluted 1:20), 0.2 µM gene-specific primer (Suppl. Table S1), and GoTaq® qPCR Master Mix (Promega, Madison, Wisconsin, USA). Gene expression level was normalized using *Mi18S* and *MiGAPDH* as endogenous reference genes. Three biological replicates were used for each treatment. All cDNA samples were carried out in technical triplicate, while primer efficiencies were previously determined, and target-specific amplification was confirmed by a single and distinct peak in the melting curve analysis. The relative expression level was calculated using the $2^{-\Delta\Delta CT}$ method (Pfaffl 2001). Data were subjected to variance analysis (ANOVA) and, when significant, means were compared by Tukey test ($P < 0.05$) using the SASM-Agri statistical package (Canteri et al. 2001).

Binary vector construction, plant transformation, and selection of transgenic plants

The vector backbone used in this study was derived from the pPZP-201BK-EGFP binary cloning vector (Chu et al. 2014), in which the T-DNA sequence (*pUceS8.3::Minc16803-dsRNA*) was cloned. In this T-DNA, the interfering dsRNA targeting *Minc16803* gene transcripts was expressed under the control of the constitutive soybean *ubiquitin-conjugating 4* promoter (*pUceS8.3*) (patent: EP1953232B1). The nucleotide sequence of the *Minc16803* gene selected to target its transcripts by the RNAi strategy corresponded to the 200 bp sequence at nucleotide positions + 445 to + 644 relative to the start codon of the *Minc16803* coding sequence. Multiple sequence alignments were used to investigate whether this 200 bp sequence can also target the two paralogous genes (Suppl. File S2). In addition, the *Minc16803* nucleotide and protein sequences were previously subjected to a similarity search with the *A. thaliana* transcriptome to make sure that no homology was present and thus avoid possible off-target effects. The sense and antisense strands of the 200 bp dsRNA cloned between *Sal*I and *Spe*I restriction sites were separated by the *pdk* intron sequence of *pyruvate orthophosphate dikinase* (Smith et al. 2000). This full-length T-DNA was synthesized and assembled into the pPZP-201BK-EGFP backbone by the Epoch Life Science (Sugar Land, Texas, EUA). Subsequently, this resulting binary vector (named GS62658-4 vir*Minc16803*) was transfected into *Escherichia coli* and then, into *Agrobacterium tumefaciens* strain GV3101.

Arabidopsis thaliana ecotype Columbia (Col-0) plants were grown to the reproductive stage on a commercial substrate in a growth room (22 °C, 70–75% relative humidity, and photoperiod 16 h with ~ 200 µmol photons $m^{-2}.s^{-1}$ of light intensity). Transgenic plants were generated using the floral dip method as described previously by Clough and Bent (1998). Then, T_1 seeds from four independent transgenic lines (Line #1 to #4) and non-transgenic (wild-type or WT) *A. thaliana* were harvested. For generation advancement, seeds were surface-sterilized with 70% ethanol for 1 min and then, with 2% sodium hypochlorite solution supplemented with 0.5% Tween-20 for 10 min. After washing the seeds five times with sterile water, they were sowed on Petri plates containing Murashige-Skoog (MS) medium (Murashige and Skoog 1962) (2.2 g MS salts, 3 g phytagel, 10 g sucrose, pH 5.7) supplemented with 15 mg/L hygromycin B (Invitrogen, Carlsbad, CA, USA), except for seeds from wild-type control plants. Seed dormancy was broken by incubating the plates for 2 days at 4 °C in the dark. Posteriorly, these plates were transferred to a growth room, and 1-week-old seedlings were transplanted to pots containing sterile commercial substrate and maintained under the same conditions as described above.

Genomic DNA was isolated from young leaves collected from *A. thaliana* plants following the CTAB/chloroform extraction method (Allen et al. 2006). DNA concentration and purity were analyzed in a NanoDrop ND-1000 spectrophotometer (NanoDrop Technologies) and 1% agarose gel electrophoresis. The screening of T_1 lines and subsequent generations (T_2 and T_3) was carried out via PCR using specific primers for detection of the *eGFP* transgene (Suppl. Table S1). PCR was performed using GoTaq® DNA polymerase (Promega, Madison, WI, USA) with a final primer concentration of 10 mM and 100 ng of genomic DNA as

template in a PCR System 9700 (Life Technologies, Carlsbad, CA, USA). The PCR conditions included an initial denaturation step at 94 °C for 2 min; 35 cycles of denaturation at 94 °C for 30 s, annealing at 60 °C for 30 s, and extension at 72 °C for 60 s, followed by a final extension at 72 °C for 5 min using a PCR System 9700 (Life Technologies, Carlsbad, CA, USA). PCR products were then analyzed in 1% agarose gel electrophoresis. Additionally, the expression of the *eGFP* reporter gene was confirmed by visualization of the eGFP fluorescence protein in seedlings under the Axio Zoom macroscope v. 16, filter set 38 HE (Carl Zeiss, Jena, Germany). Segregation analyses of *A. thaliana* lines were performed based on inheritance patterns analyzed by germination of surface-sterilized seeds onto Petri plates containing MS medium supplemented with 15 mg/L hygromycin B up to the T_3 generation. Four independents transgenic T_3 lines were randomly selected to be used in nematode infection bioassays.

Meloidogyne incognita infection assay

For nematode infection bioassays of transgenic *A. thaliana* lines (Line #1 to #4) and wild-type control plants, 20-day-old plants were inoculated with 500 ppJ2s and maintained in a growth room at 22 °C. The *A. thaliana* plants were harvested at 60 DAI; roots were washed with water and stained with floxin B (Taylor and Sasser 1987). Then, galls and egg masses were counted and dissected under a binocular microscope, and the reproduction ratio [number of egg masses/number of galls] was evaluated. The bioassay was carried out with 10 plants per transgenic line or wild-type control *A. thaliana* in two biological repetitions.

Minc16803-RNAi transgene expression and *Minc16803* gene downregulation in *M. incognita* during parasitism in transgenic *A. thaliana* lines

Total RNA was extracted from transgenic and wild-type seedlings or galls at 10 DAI using TRIzol (Life Technologies, Carlsbad, CA, USA) according to the manufacturer's recommendations. RNAi transgene expression in transgenic *A. thaliana* lines was confirmed by RT-qPCR analysis using specific primers for the *pdk* intron sequence. Relative expression of the RNAi transgene was normalized using *AtActin 2*, *AtGAPDH*, and *AtEF1* as reference genes (Suppl. Table S1) and calibrated to the levels of the Line #1. On the other hand, *Minc16803* gene downregulation in *M. incognita* during its parasitism in transgenic *A. thaliana* lines was confirmed by RT-qPCR analysis using *MiGAPDH*, *MiActin* and *Miβ-tubulin* as reference genes (Suppl. Table S1). Primer efficiency was calculated using the Miner tool (http://www.miner.ewindup.info), and relative gene expression was analyzed using the $2^{-\Delta\Delta CT}$ method (Pfaffl 2001) through qBase + v.3.1 software (Biogazelle, Zwijnaarde, Belgium). The suitability of the *A. thaliana* and *M. incognita* reference genes was evaluated by geNorm analysis (Vandesompele et al. 2002), which showed *M-values* below 0.5. Each treatment consisted of three biological replicates and each biological replicate included three to five plants. All samples were evaluated in technical triplicates.

Gall morphology analysis of wild-type and transgenic *A. thaliana* lines

Galls of transgenic lines and wild-type control plants were collected at 7, 21 and 45 DAI, fixed in 2% glutaraldehyde in 50 mM PIPES buffer pH 6.9 for 15 days, dehydrated with an ethanol gradient (15, 30, 50, 70, 80, and 100%), embedded and polymerized in Technovit™ 7100 (Kulzer, Friedrichsdorf, Germany) as described by the manufacturer. Galls were then sectioned (3 µm), stained in 0.05% (w/v) toluidine blue, and mounted with Depex (Sigma-Aldrich, St. Louis, MO, USA). For morphological analyses, stained sections were observed under bright-field light microscopy, and the images were obtained with a digital camera (AxiocamHRc, Carl Zeiss, Oberkochen, Germany). At least 50 sections from 30 different galls of transgenic or wild-type control plants were analyzed. The mean diameter of galls and mean area of feeding sites were measured with ZEISS ZEN software. A total of 30 galls from two different experiments were examined per treatment.

Results

Bioinformatics analysis of *Minc16803* gene

Using different bioinformatics filters detailed in the methods section, we identified a putative effector gene in the *M. incognita* genome, referred here as *Minc16803* gene, located in the *Minc3s00746g16803* locus. The *Minc16803* gene is approximately 1.66 kb in size, divided into 10 exons and 9 intron sequences, and flanked by 5'- and 3'-UTR sequences. Its CDS sequence has 1,052 nucleotides encoding a protein of 343 amino acids, a predicted isoelectric point of 9.2, and a molecular weight of 40.25 kDa (Table 1; Suppl. File S1). The Minc16803 protein sequence showed the presence of a secretory signal peptide (from position 1 to 22 amino acid) at the N-terminal portion, a predicted non-cytoplasmatic domain, and the absence of transmembrane motifs, indicating that Minc16803 is likely a secreted protein (Table 1). In a previous analysis, four degenerate protein motifs had been identified enriched at the N-terminal region of known *M. incognita* effectors (Vens et al. 2011). We found three of

Table 1 Features of *Minc16803* (*Minc3s00746g16803*) gene, its two paralogous *Minc3s00200g07395* and *Minc3s00070g03473* genes, and its potential orthologous genes in other nematode species. The gene sequences were retrieved from WormBase database version WBPS16

Nematode species	Gene ID	Gene description	Nucleotide	Amino acid	Gene expression	Protein immunolocalization	CDD domain	PFAM domain	NLS motif	Signal peptide
M. incognita	*Minc3s00746g16803 Minc16803*	Putative effector involved in parasitism	1052	343	All nematode stages	Undefined	No	Non-cytoplasmatic domain	No	Yes
M. incognita	*Minc3s00200g07395*	*Minc16803* paralog	957	311	All nematode stages	Undefined	No	Non-cytoplasmatic and transmembrane domains	No	Yes
M. incognita	*Minc3s00070g03473*	*Minc16803* paralog	1099	292	All nematode stages	Undefined	No	Non-cytoplasmatic domain	No	Yes
M. floridensis	*scf7180000420581*	Orthologue of the *Minc16803*	937	312	Undefined	Undefined	No	No	No	No
M. javanica	*scaffold37606_cov431.g23340*	Orthologue of the *Minc16803*	804	267	Undefined	Undefined	No	Non-cytoplasmatic domain	No	Yes
M. hapla	*MhA1_Contig468.frz3.gene9*	Orthologue of the *Minc16803*	648	215	Undefined	Undefined	PLN02286	IPR001278	No	No
M. hapla	*MhA1_Contig468.frz3.gene5*	Orthologue of the *Minc16803*	870	289	Undefined	Undefined	No	Non-cytoplasmatic domain	No	Yes
G. rostochiensis	*GROS_g05191*	Orthologue of the *Minc16803*	1413	470	Undefined	Undefined	No	Non-cytoplasmatic domain	Yes	Yes
G. pallida	*GPLIN_000992700*	Orthologue of the *Minc16803*	1206	401	Undefined	Undefined	No	No	Yes	No
D. destructor	*Dd_04152*	Orthologue of the *Minc16803*	1548	515	Undefined	Undefined	No	No	Yes	No
B. xylophilus	*BXYJ5.050084300*	Orthologue of the *Minc16803*	1152	383	Undefined	Undefined	No	Non-cytoplasmatic domain	Yes	Yes
Bursaphelenchus okinawaensis	*BOKI.050088700*	Orthologue of the *Minc16803*	1170	389	Undefined	Undefined	No	Non-cytoplasmatic domain and signal peptide	Yes	Yes
Bursaphelenchus xylophilus	*BXY_0398000*	Orthologue of the *Minc16803*	1152	383	Undefined	Undefined	No	Non-cytoplasmatic domain and signal peptide	Yes	Yes
Ditylenchus dipsaci	*jg3035*	Orthologue of the *Minc16803*	795	264	Undefined	Undefined	No	No	Yes	No
Heterodera glycines	*Hetgly17661*	Orthologue of the *Minc16803*	1979	488	Undefined	Undefined	No	signal peptide	Yes	Yes

Table 1 (continued)

Nematode species	Gene ID	Gene description	Nucleotide	Amino acid	Gene expression	Protein immunolocalization	CDD domain	PFAM domain	NLS motif	Signal peptide
Heterodera schachtii	*Hsc_gene_10797*	Orthologue of the *Minc16803*	1470	489	Undefined	Undefined	No	Non-cytoplasmatic domain and signal peptide	Yes	Yes
Meloidogyne graminicola	*NXFT01001968.1.5091_g*	Orthologue of the *Minc16803*	600	199	Undefined	Undefined	No	No	No	No

PLN02286 Arginine-tRNA ligase, *IPR001278* Arginine-tRNA ligase

these four motifs at the N-terminal region of the encoded protein sequence of Minc16803 and Minc3s00070g03473, providing additional evidence that they might be putative *M. incognita* effectors. However, Minc3s00200g07395 did not show any of the degenerate motifs (Fig. 1A, Suppl. Table S2).

We also retrieved and analyzed the phylogenetic tree corresponding to gene entry 'Minc3s00746g16803' in WormBase Parasite (https://parasite.wormbase.org/Multi/GeneTree/Image?gt=WBGT00000000029539). All phylogenetic trees in WormBase Parasite have been generated using Ensembl Compara pipeline (Cunningham et al. 2022), which produces both nucleotide and amino acid-based phylogenies and then, compare to a reference species tree to infer duplication and speciation branches and thus, orthology and paralogy. The phylogenetic tree for *Minc16803* confirmed that *Minc3s00070g03473* and *Minc3s00200g07395* can be consistently considered its paralogs (Fig. 1B). In addition, orthologs were identified in several other species albeit all being plant-parasitic nematodes, including other root-knot nematodes (*Meloidogyne floridensis, Meloidogyne hapla, M. graminicola,* and *M. javanica*), cyst nematodes (*Globodera pallida*, *Globodera rostochiensis*, *H. glycines* and *Heterodera schachtii*), stem and bulb nematode (*Ditylenchus dipsaci*), and the pine wilt nematodes (*Bursaphelenchus xylophilus* and *Bursaphelenchus okinawaensis*). Therefore, *Minc16803* is widely conserved in several plant-parasitic nematodes, but specific to phytoparasites (Table 1, Fig. 1B). The high sequence identity between *Minc16803* and its two paralogous genes (95 to 99% amino acid identity) suggests that they may likely be the result of gene duplication, consistent with the triploid structure of the *M. incognita* genome (Blanc-Mathieu et al. 2017).

Minc16803 expression level at different *M. incognita* developmental stages

From transcriptome data mining, it was possible to identify the *Minc16803* gene expression profile, as well as its two paralogous *Minc3s00070g03473* and *Minc3s00200g07395* genes, at different *M. incognita* life stages (egg, ppJ2, pJ2/J3, J4, and female) during nematode parasitism in plants (Fig. 1C). Interestingly, the expression of all three genes was similar across the five different life stages of *M. incognita*; however, the *Minc3s00200g07395* gene had a higher expression level than the other genes at all developmental stages (Fig. 1C). Then, the in silico *Minc16803* gene expression data were confirmed by RT-qPCR analysis in different developmental stages of *M. incognita* during infection in *N. tabacum* plants. The different stages of the nematodes collected for the RT-qPCR analysis were identified through acid fuchsin staining of tobacco roots infected with *M. incognita*. Under our experimental conditions, penetration of ppJ2

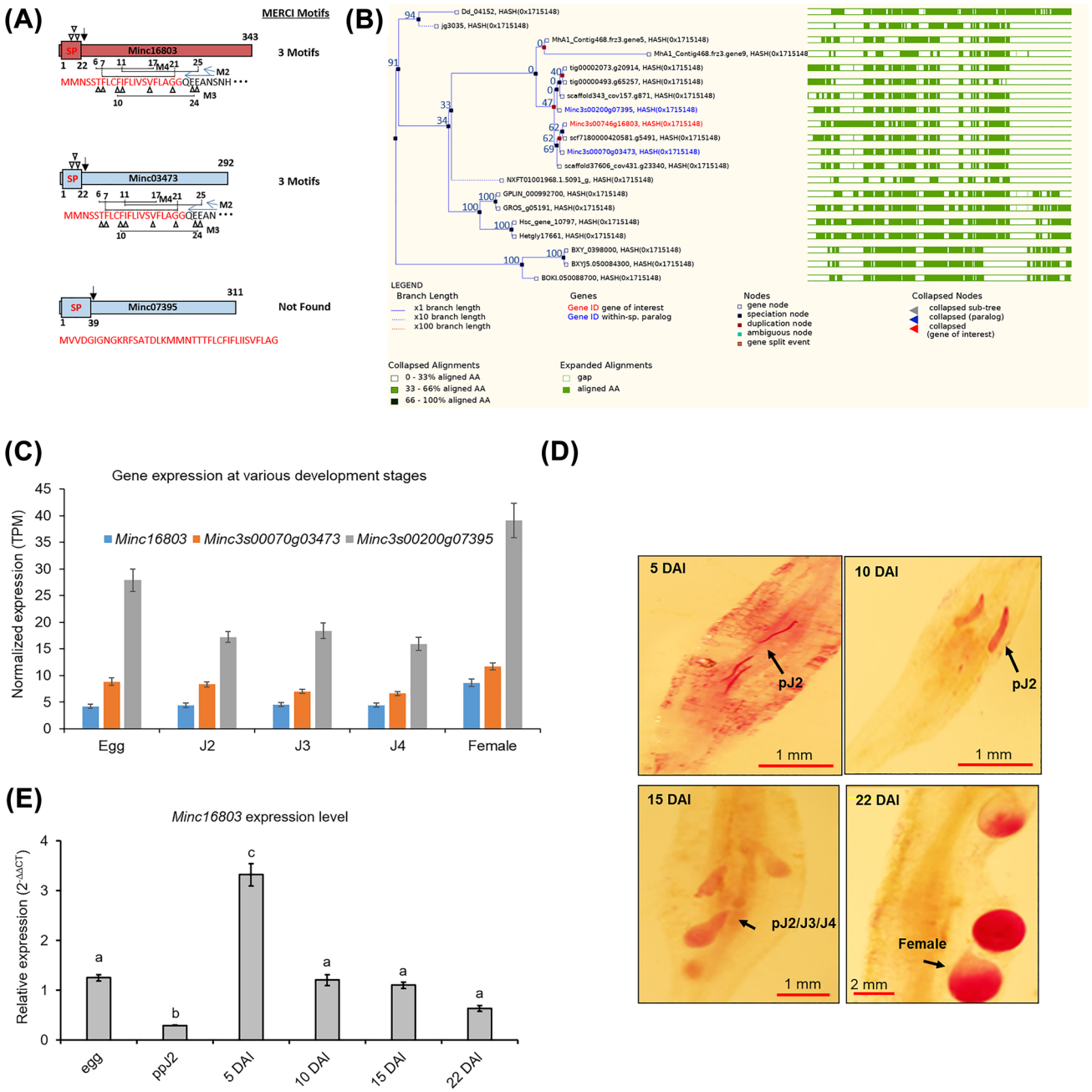

Fig. 1 Sequence analysis and gene expression profiles. **A** Schematic representation of MERCI motifs found at the N-terminal region of Minc16803 and Minc3s00070g03473 proteins. **B** Final merged phylogenetic tree (WBGT00000000029539), corresponding to *Minc16803* as well as its paralogs and orthologs retrieved from WormBase Parasite. **C** Gene expression profiles of the *Minc16803* and its paralogs *Minc3s00200g07395* and *Minc3s00070g03473* genes at different *M. incognita* life stages: egg, pJ2, J3, J4, and female, retrieved from WormBase Parasite and based on transcriptome datasets under BioProject number PRJNA390559 (Choi et al. 2017). Error bars represent confidence intervals corresponding to three libraries per nematode life stage. **D** Histological images of *M. incognita* pJ2, pJ2/J3/J4, and female during parasitism in *N. tabacum* roots at 5, 10, 15, and 22 days after inoculation (DAI). **E** *Minc16803* gene expression profile measured by RT-qPCR analysis in different *M. incognita* life stages (egg, ppJ2, and pJ2 to female) during its parasitism in *N. tabacum*. Relative expression levels were normalized with *Mi18S* and *MiGAPDH* as endogenous reference genes. Data are presented as means ± SE of three biological replicates. Different letters on the bars indicate significant differences based on Tukey's test ($P < 0.05$)

infectious juveniles into the root tissue starts within 1 DAI. Juvenile nematode migration toward the vascular cylinder is mainly visible around 5 DAI (Fig. 1D), and nematodes are characterized by a vermiform and slender body shape.

At 10 and 15 DAI, we verified that most tobacco roots were infected by *M. incognita,* presenting a more swollen body shape, and numerous nematodes were observed nearby the vascular tissue during the induction and establishment of feeding sites (Fig. 1D). The infected region shows clear changes in morphology, forming swellings and the typical fully developed galls around 15 DAI. However, it was not possible to precisely characterize the development stage of nematodes at 10 and 15 DAI based on their morphology due to the presence of pJ2 and non-feeding J3 and J4 nematodes. At 22 DAI, several adult females displaying a pear-shaped body were clearly observed in developed galls within the roots (Fig. 1D). We observed a significant decrease in the transcript levels of *Minc16803* in ppJ2 and at 22 DAI, while at 10 and 15 DAI, the *Minc16803* expression was similar to that observed in the eggs stage. The highest *Minc16803* expression was observed in pJ2 at 5 DAI, with an increase of 2.65-fold compared to the eggs, suggesting that the *Minc16803* plays a role at the early stages of parasitism (Fig. 1E).

Transgenic *A. thaliana* lines harboring *Minc16803*-dsRNA

To investigate the effect of *in planta* expression of dsRNA targeting *Minc16803* on *M. incognita* parasitism, several transgenic *A. thaliana* lines were generated. Then, we randomly selected only four lines (Line #1 to #4) for further analysis. The 200 bp sequence of the *Minc16803* transcript was cloned in sense and antisense separated by the *pdk* intron sequence in an expression cassette controlled by the strong and constitutive *pUceS8.3* promoter (Fig. 2A). In silico analysis using si-Fi software (Lück et al. 2019) revealed that the *Minc16803*-dsRNA designed based on 200 bp *Minc16803* sequence was predicted to generate 84 and 32 perfect matching 21 nucleotides small-interfering RNA (siRNA) molecules against its paralogous *Minc3s00070g03473* and *Minc3s00200g07395* genes, respectively. This data indicated that *Minc16803* and its two paralogous could be downregulated by the RNAi sequence used here, possibly resulting in the disruption of their biological function. After floral dip transformation, *A. thaliana* plants resistant to hygromycin were characterized by PCR to confirm the insertion of the T-DNA into the plant nuclear genome in T_1 to T_3 generations. Transgenic plants were also selected in MS medium supplemented with 15 mg/L hygromycin B up to T_3 generation, and an uniform population of resistant seedlings in the progenies was observed (Fig. S1A). Amplification by PCR of the *eGFP* fragment (423 bp) over the three generations demonstrated stable inheritance of the T-DNA (Fig. 2B). Additionally, the transgenic events were also confirmed by confocal analyses of eGFP fluorescence protein accumulation in the plant leaves (Fig. 2C). Phenotypic differences between the transgenic lines and wild-type control plants were not identified, indicating that the expression of *Minc16803*-dsRNA did not result in pleiotropic effects on plant architecture and development (Suppl. Fig. S1B).

Meloidogyne incognita infection assay on transgenic *A. thaliana* lines

To evaluate the efficacy of *in planta Minc16803*-dsRNA overexpression in reducing plant susceptibility to *M. incognita*, bioassays using *M. incognita* race 3 inoculum were performed with four transgenic lines and wild-type plants. Then, these plants were evaluated for galls/plant and egg masses/plant. Consistently, we observed a significant reduction of 66.3–84% in the number of galls and 79.3–93.3% in egg masses in transgenic *A. thaliana* lines compared with wild-type plants (Fig. 2D, E). Further, a significant decrease in the ratio [number of egg masses/number of galls] ranging from 54.7 to 64.1% was verified in the transgenic lines (Fig. 2F). Subsequently, RT-qPCR analyses were performed to confirm that the transgenic lines successfully overexpressed *Minc16803*-dsRNA and to examine whether the observed effects on nematode parasitism were due to *Minc16803* gene downregulation. Transgene expression analyses targeting the *pdk* intron showed that *Minc16803*-dsRNA was overexpressed in all four transgenic lines, whereas in the wild-type plants, gene expression was not detected (Fig. 2G). In addition, a significant decrease in *Minc16803* gene expression of 90–95% was observed in nematodes during parasitism in transgenic lines compared to those in wild-type control plants (Fig. 2H). However, our attempts to determine the silencing of *Minc3s00070g03473* and *Minc3s00200g07395* were unsuccessful. Due to the high identity among *Minc16803*, *Minc3s00070g03473,* and *Minc3s00200g07395*, it was not possible to design specific and efficient primers to detect *Minc3s00070g03473* and *Minc3s00200g07395* expression. We designed four pairs of primers for each gene (*Minc3s00070g03473* and *Minc3s00200g07395*), but all of them had poor performance. Primers that did not amplify the target sequence or primers that amplified the target sequence with efficiencies outside the acceptable range to be considered suitable for RT-qPCR analyses (90–110%) and/or showed more than one PCR amplification peak according to melting curve analysis were considered primers with poor performance.

Histological analysis of the galls in the transgenic *A. thaliana* lines

To further characterize the effects of *Minc16803* gene downregulation on nematode during plant parasitism, transgenic *A. thaliana* plants from Line #1 and wild-type control plants were infected with *M. incognita* ppJ2, and the roots were

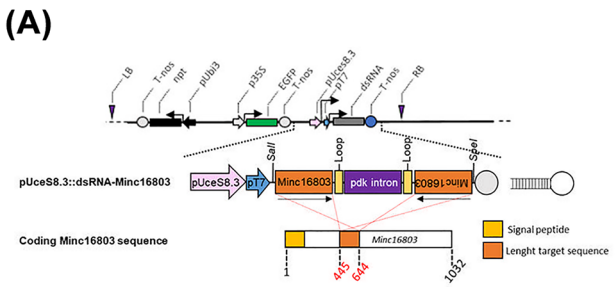
(A)
LB
T-nos
npt
pUbi3
p35S
EGFP
T-nos
pUceS8.3
pT7
dsRNA
T-nos
RB
pUceS8.3::dsRNA-Minc16803
pUceS8.3
pT7
Minc16803
pdk intron
Minc16803
SalI
SstI
Loop
Loop
Coding Minc16803 sequence
Minc16803
Signal peptide
Lenght target sequence
1
445
644
1032

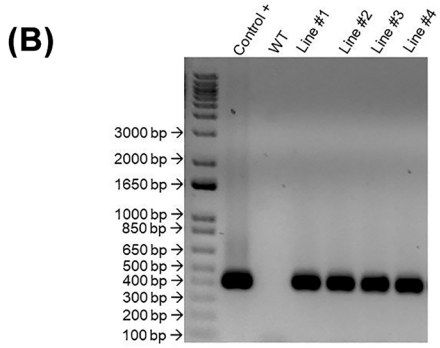
(B)
Control +
WT
Line #1
Line #2
Line #3
Line #4
3000 bp
2000 bp
1650 bp
1000 bp
850 bp
650 bp
500 bp
400 bp
300 bp
200 bp
100 bp

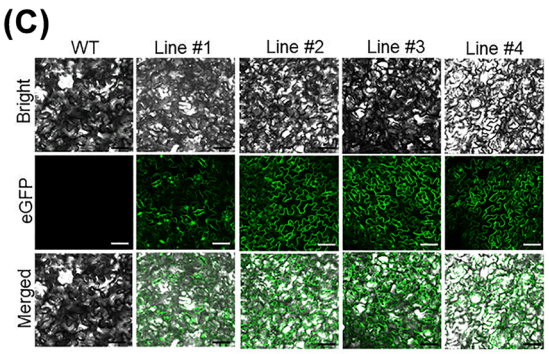
(C)
WT
Line #1
Line #2
Line #3
Line #4
Bright
eGFP
Merged

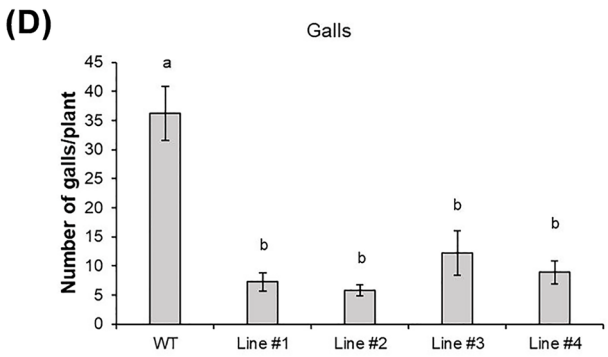
(D)
Galls
Number of galls/plant
a
b
b
b
b
WT
Line #1
Line #2
Line #3
Line #4

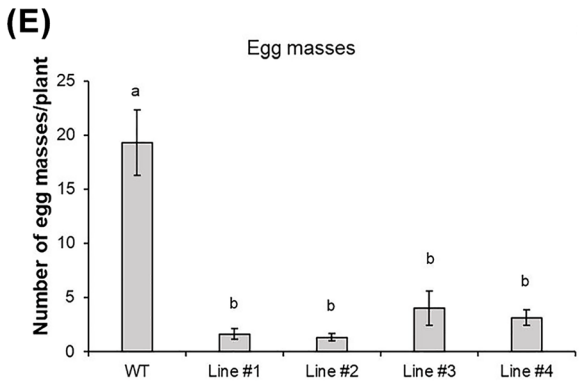
(E)
Egg masses
Number of egg masses/plant
a
b
b
b
b
WT
Line #1
Line #2
Line #3
Line #4

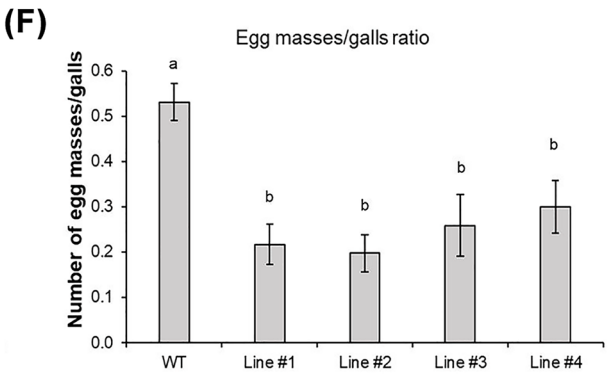
(F)
Egg masses/galls ratio
Number of egg masses/galls
a
b
b
b
b
WT
Line #1
Line #2
Line #3
Line #4

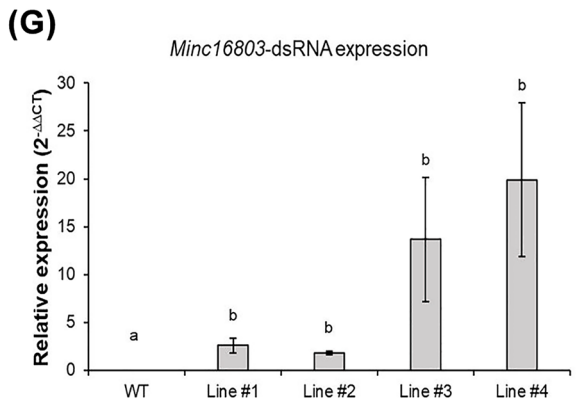
(G)
Minc16803-dsRNA expression
Relative expression (2-ΔΔCT)
a
b
b
b
b
WT
Line #1
Line #2
Line #3
Line #4

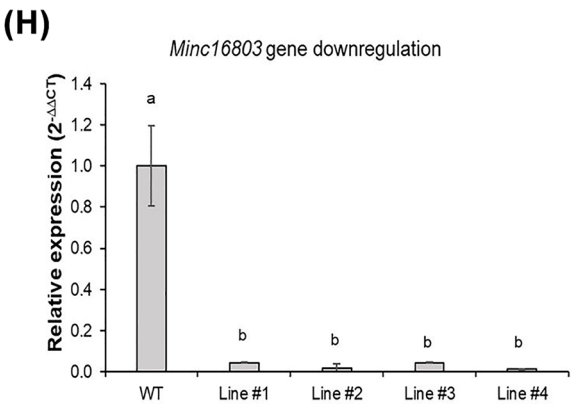
(H)
Minc16803 gene downregulation
Relative expression (2-ΔΔCT)
a
b
b
b
b
WT
Line #1
Line #2
Line #3
Line #4

◂**Fig. 2** *Agrobacterium*-mediated genetic transformation of *A. thaliana*, susceptibility level of transgenic *A. thaliana* lines to *M. incognita* race 3, and *Minc16803* gene expression in *M. incognita* during its parasitism in transgenic lines and wild-type control plants. **A** Overview of the T-DNA used into binary vector for genetic transformation of *A. thaliana* plants, targeting downregulation of *Minc16803* gene transcripts by the *in planta* RNAi strategy. **B** PCR detection of the *eGFP* transgene in *A. thaliana* lines, indicating the expected amplicon size of 400 bp. Marker: 1.0-kb DNA ladder (Invitrogen); positive control: binary vector; WT: wild-type control plant used as a negative control for PCR analysis and plant-nematode bioassays. **C** Fluorescence detection of eGFP protein in transgenic lines under a Zeiss inverted LSM510 META laser scanning microscope using 488-nm excitation line and the 500–530-nm band pass filter (Carl Zeiss). Scale bars: 10 mm. Plant susceptibility analysis based on **D** number of galls per plant, **E** number of egg masses per plant, and **F** ratio [number of egg masses/number of galls] in T_3 transgenic *A. thaliana* lines ($n = 10$ plants) at 60 DAI. Data are presented as means ± SE of 10 plants per transgenic line or wild-type control. Different letters on bars indicate statistically significant differences according to Tukey's test ($P < 0.05$). **G** Transgene expression level measured by RT-qPCR analysis in transgenic lines and wild-type control plants using the *pdk* intron fragment as the target. Relative expression levels were normalized using *AtActin 2*, *AtGAPDH,* and *AtEF1A* as endogenous reference genes. Transgene expression was undetected in WT plants, and transgene expression levels were relative to the expression of Line #1. **H** *Minc16803* gene expression measured by RT-qPCR analysis in *M. incognita* during parasitism in transgenic lines and wild-type control plants. Relative expression levels were normalized with *MiActin, MiTubulin* and *MiGAPDH* as endogenous reference genes. Data are presented as means ± SE of three biological replicates. Different letters on the bars indicate significant differences based on Tukey's test ($P < 0.05$)

collected at 7, 21, and 45 DAI for histological analysis. This analysis was focused only on Line #1 because it showed similar susceptibility levels to *Minc16803*-dsRNA Lines #2, #3, and #4 (Fig. 2D, F). We observed that the galls collected at 7 and 21 DAI in the wild-type plants showed maturing nematodes and multiple well-developed feeding sites with giant cells containing a dense cytoplasm, while upon *Minc16803* downregulation, giant cells were devoid of cytoplasm and nematodes showed morphological alterations (Fig. 3A, B).

The wild-type control roots at 45 DAI showed a large number of galls containing giant cells filled with cytoplasm and mature nematodes that developed normally. In addition, egg-laying females were often visible at 45 DAI (Fig. 4A). *Minc16803*-dsRNA (Line #1) infected roots showed fewer and smaller galls compared to wild-type roots. In *Minc16803*-dsRNA galls, we observed malformed nematodes without well-defined shapes, which stained more intensely than nematode sections in the wild-type plants (Fig. 4B). This suggests that induced downregulation of *Minc16803* within nematodes strongly affected their development and likely their maturation. However, some nematodes were capable of laying eggs that often hatched before egg mass extrusion (Fig. 4B). In addition, the gall diameters at 7 and 45 DAI, as well as the feeding site areas at 45 DAI from *Minc16803*-dsRNA (Line #1) roots, were significantly smaller compared to those from wild-type roots (Fig. 4C, D, E).

Discussion

Meloidogyne incognita is among the most devastating PPNs and has caused severe yield losses to several crops worldwide (Bernard et al. 2017). Currently, the control of *M. incognita* is mainly based on the use of chemical nematicides and resistant cultivars developed through conventional breeding (Koenning et al. 2001; Wheeler et al. 2014). However, *M. incognita* continues to overcome the limited number of resistant cultivars available, and several nematicides have been banned from use or are being phased out due to their negative impact on the environment and human health (Zhou et al. 2000; Silva et al. 2014; Oka 2020). Therefore, the development of innovative and environmentally friendly strategies for managing *M. incognita* is crucial to promote more sustainable agricultural systems.

Meloidogyne incognita has developed sophisticated mechanisms of parasitism to manipulate plant physiology and immunity signaling pathways that ultimately result in the establishment of permanent feeding structures, whereby nematodes take up nutrients needed for their development and reproduction (Kyndt et al. 2013; Ali et al. 2017). Among these, effector-dependent parasitism mechanisms are pivotal for successful infection during compatible plant-nematode interactions (Mejias et al. 2019). Identifying novel *M. incognita* target genes that encode effector proteins is an important step toward developing innovative biotechnological strategies that can be applied to the management of this devastating plant-parasite (Rutter et al. 2014). Herein, we described the identification of the *Minc16803* putative effector gene and demonstrated its contribution to the enhancement of *A. thaliana* resistance to *M. incognita* through the host-induced gene silencing system.

With rapid advances in sequencing technologies, genomic and transcriptomic information from an increasing number of nematodes is becoming available, which has facilitated the prediction and characterization of numerous effectors (Danchin et al. 2013; Pogorelko et al. 2020; Grynberg et al. 2020; Rocha et al. 2021). Prior to functional analyses, the prediction of putative effectors relies primarily on in silico analysis of genes encoding proteinaceous secretions that have a signal peptide for secretion and the absence of transmembrane domains (Xie et al. 2016; Chen et al. 2017). Taking advantage of published genomes for *M. incognita*, we identified the *Minc16803* gene. At a first step, an assessment of protein sequence using bioinformatic analyses was performed. As expected, we found that the predicted protein encoded by the *Minc16803* gene retrieved from the *M. incognita* genome contains a signal peptide and lacks

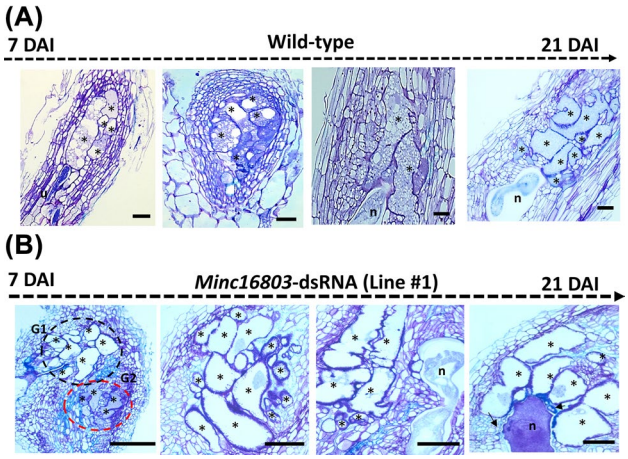

Fig. 3 Histological analysis of galls in wild-type and transgenic plants infected with *M. incognita*. Gall sections were stained with toluidine blue and imaged by bright-field microscopy. **A** Galls sections in the wild-type control roots showed well-developed feeding sites and nematodes. **B** *Minc16803*-dsRNA (Line #1) transgenic galls showed giant cells with low cytoplasmic content and apparent unstructured nematodes. Note that nematodes cuticle seems affected, and nematodes stained more strongly, suggesting morphological changes during their development (black arrows). *, giant cell; n, nematode; G1, gall 1 and G2, gall 2. Scale bars: 50 µm

transmembrane domains, which is structurally consistent with the potential secretory nature of the protein. The N-terminal signal peptide is important for directing the effector proteins from the cytoplasm to the endoplasmic reticulum of the nematode secretory esophageal gland cells, and then, the mature effector proteins are secreted into the root cells via the nematode stylet (Wang et al. 2010). Accordingly, the Minc16803 protein is presumably secreted. In addition, three motifs typical of known effectors (Vens et al. 2011; Grynberg et al. 2020; Rocha et al. 2021) were identified in the predicted Minc16803 protein sequence, suggesting that Minc16803 might be an effector protein secreted in plant tissue during parasitism. However, future in situ hybridization and/or antibody localization studies will be required to assess whether Minc16803 is expressed in the nematode esophageal gland cells and secreted in plant tissues in order to confirm that it is indeed an effector protein. Furthermore, putative orthologs of *Minc16803* gene were found in other *Meloidogyne* spp., as well as in other nematode genera, all being plant-parasitic species, suggesting that this gene may have a conserved role not only in the parasitism of *Meloidogyne* spp. but also in other phytoparasitic nematodes.

Subsequently, we analyzed the expression level of *Minc16803* gene throughout the life cycle of *M. incognita* during the compatible *M. incognita*-tobacco interaction. The peak of *Minc16803* gene expression at 5 DAI suggests that this putative effector acts at the early stages of infection by interfering with the initiation and/or establishment

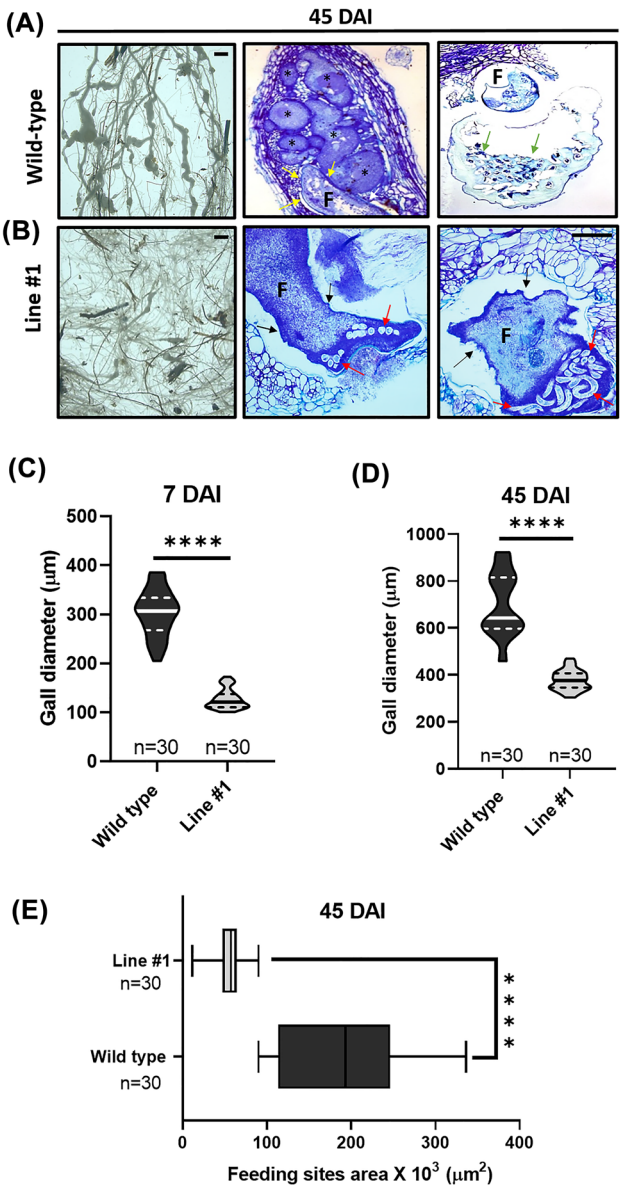

Fig. 4 Histological analysis of *M. incognita*-induced galls and measurement of the galls and feeding sites. Gall sections were stained with toluidine blue and imaged by bright-field microscopy. **A** Wild-type control roots illustrated a large number of galls at 45 DAI containing giant cells filled with cytoplasm. Nematodes had a rounded form and cuticles less stained (yellow arrows). Egg-laying females and egg masses (green arrows) were often visible at 45 DAI. **B** *Minc16803*-dsRNA (Line #1) infected roots showed fewer and smaller galls compared to wild-type roots. In *Minc16803*-dsRNA galls, the nematodes illustrated irregular forms and the cuticle seemed altered (black arrows), with no well-defined morphology and nematodes stained more strongly, suggesting structural body changes. Strikingly, the eggs in *Minc16803*-dsRNA (Line #1) apparently hatched prematurely (red arrows) compared to what was seen in wild-type plants (green arrows), and the gelatinous matrix containing the eggs colored more strongly. **C–D** Gall diameter measurements revealed significantly smaller galls in *Minc16803*-dsRNA (Line #1) compared to wild-type galls at 7 DAI and 45 DAI. **E** Feeding site area measurements revealed significantly smaller feeding sites in *Minc16803*-dsRNA (Line #1) compared to those in wild-type galls at 45 DAI. This analysis demonstrated that *Minc16803* down-regulation had a direct effect on gall and nematode development. Data are presented as means ± SD from two experiments with $n = 30$ galls examined per treatment. Statistical differences between treatments are based on Student`s t test (****$P < 0.0001$). *, giant cell; n, nematode; *F*, female. Scale bars: 50 µm

of feeding sites. However, *Minc16803* and its two paralogous genes were found to have considerable expression levels in all stages of nematode development. Suppression of plant defense at the early stages of nematode infection is extremely important to establish a successful infection. Thus, nematodes are expected to use some effectors at the early stages of parasitism, which is supported by the upregulation of the *Minc16803* gene at 5 DAI. Similar to our results, the *MjTTL5*, *MgGPP*, and *Mi-msp2* effector genes have been shown to be upregulated at early stages of *M. javanica*, *M. graminicola*, and *M. incognita* parasitism, respectively (Lin et al. 2016; Chen et al. 2017; Joshi et al. 2019).

In addition, an infection bioassay was performed to test whether the transgenic *A. thaliana* lines expressing *Minc16803*-dsRNA affect the infection and reproduction process of *M. incognita.* Indeed, the expression of *Minc16803*-dsRNA in transgenic *A. thaliana* lines downregulated *Minc16803* transcripts in the nematode, leading to reduced susceptibility of plants to *M. incognita*. We observed that the T_3 progeny of four independent transgenic lines showed a significant decrease of up to 84% and 93.3% in the number of galls and number of egg masses, respectively, indicating that *Minc16803* gene downregulation not only affected the ability of the nematode to infect the host plant but also compromised nematode reproduction. Furthermore, it was found that the ratio of number of egg masses/number of galls was significantly lower in the transgenic lines compared with the wild-type control plants. These data strongly suggest that the significant downregulation of *Minc16803* transcripts compromised the development of later-stage juveniles into female adults, as well as egg production that could ensure novel galls establishment. Thus, the reduced plant susceptibility to *M. incognita* among the four transgenic lines was most likely associated with the *Minc16803* gene expression downregulation in nematodes and potentially of its two paralogous genes.

In agreement with our findings that Minc16803 protein is critical for *M. incognita* infection and reproduction, a recent study showed that the number of galls in transgenic *A. thaliana* plants overexpressing dsRNA molecules against the effector genes *Mi-msp3*, *Mi-msp5*, *Mi-msp18,* and *Mi-msp24* of *M. incognita* was reduced by 89%, 78%, 86%, and 89%, respectively. In addition, the reproduction factor was significantly reduced in all dsRNA-overexpressing lines compared to the wild-type control plants (Joshi et al. 2020). Likewise, downregulation of the *Mi-msp2* effector gene by RNAi was shown to reduce *A. thaliana* susceptibility to *M. incognita*, as observed by the significant reduction in the number of galls, females, and egg masses by up to 54%, 66%, and 95%, respectively (Joshi et al. 2019). Furthermore, dsRNA molecules that target the *MiPDI1* effector gene were found to confer reduced susceptibility to *M. incognita* when overexpressed in *A. thaliana* (Zhao et al. 2020).

Unlike insects, nematodes are able to amplify the siRNA signal by RNA-dependent RNA polymerases (Pak and Fire 2007), and therefore, even a small amount of dsRNA produced by the plant may induce strong and prolonged gene downregulation in nematode cells. In addition, the siRNAs generated by the processing of dsRNA by the plant RNAi machinery can be efficiently taken up by nematode midgut cells and trigger an RNAi response (Steeves et al. 2006). Thus, the development of RNAi-based transgenic crops against highly effective target genes offers a valuable approach for conferring resistance to phytonematodes. Several studies have shown the efficacy of host-delivered RNAi silencing of effector and essential genes to control different nematode species, including *M. incognita* (Dinh et al. 2014; Dutta et al. 2015; Chaudhary et al. 2019; Zhao et al. 2019, 2020). Interestingly, Tian et al. 2019 reported that overexpression of dsRNA molecules targeting the *H. glycines HgY25* and *HgPrp17* genes in transgenic soybean plants resulted in a significant reduction in cyst and egg numbers. Similarly, it was recently shown that simultaneous downregulation of *cysteine protease*, *isocitrate lyase*, and *splicing factor* genes significantly impaired plant parasitism by *M. incognita* in transgenic cotton lines (Lisei-de-Sá et al. 2021).

To better understand how *Minc16803* gene downregulation might affect plant-nematode interactions, histological analyses of *M. incognita*-induced galls in the transgenic *A. thaliana* line and wild-type control plants were compared. Our results demonstrated that *Minc16803* plays a role in the induction and establishment of feeding sites as the transgenic galls exhibited giant cells lacking cytoplasm and surrounded by even more asymmetrically dividing neighboring cells. Interestingly, nematodes in the transgenic lines displayed irregular body shapes, suggesting cuticle damage and cytoplasmic degeneration. The morphological alterations in the nematode body might be attributed to the fact that giant cells did not support the full development of the nematodes. Intriguingly, numerous hatching *M. incognita* ppJ2s were frequently observed in the amorphous egg mass secreted by female nematodes that remained inside the root. These alterations indicate that some females, even with an aberrant phenotype, were able to lay the eggs that apparently hatched prematurely, perhaps in an effort to accelerate their infection cycle. Therefore, it is possible that the significant reduction in the number of egg masses found on the root surface of the transgenic lines is due to the unhealthy state of the maturing nematodes.

The molecular mechanisms by which nematode effector proteins overcome plant defense systems and facilitate plant parasitism are diverse. For instance, *M. javanica* MjTTL5 effector alters the plant's oxidative response through augmentation of the host's ROS-scavenging system by interacting with *A. thaliana* ferredoxin:thioredoxin reductase catalytic subunit (Lin et al. 2016). *M. incognita* MiMIF-2

interacts with *A. thaliana* annexins to suppress host immune responses and promote parasitism (Zhao et al. 2019). On the other hand, *M. incognita* MiEFF18 has been shown to target the plant core spliceosomal protein SmD1 to modulate the expression of critical genes required for giant cell ontogenesis (Mejias et al. 2021). However, the molecular mechanisms underlying the process by which the putative Minc16803 effector suppresses plant defenses to establish parasitism remain to be investigated. In addition, detailed studies will allow the precise identification of the tissues or cells in which the putative Minc16803 effector specifically acts, and the host target proteins that interact with Minc16803.

In summary, our findings indicate that transgenic *A. thaliana* lines overexpressing a *Minc16803*-dsRNA targeting *Minc16803* transcripts have reduced susceptibility to *M. incognita,* as observed by the remarkable reduction in the number of galls and egg masses. These results suggest that the putative *Minc16803* effector gene is an amenable target for improving the resistance of economically important crops to *M. incognita* using *in planta* RNAi technology. The *Minc16803* dsRNA can be pyramided with dsRNAs targeting other nematode genes or even with plant resistance genes to develop genetically engineered crops with improved and durable resistance to *M. incognita.* Furthermore, a major advantage of using RNAi technologies is that the dsRNA molecules can be rationally designed based on the gene sequence of interest to specifically target *M. incognita* or a wider range of closely related nematode species. Given that putative *Minc16803* orthologous have been found in other *Meloidogyne* spp. and the relative flexibility in selecting *Minc16803*-dsRNA target sites based on the gene sequence, the RNAi cassette could be adapted to downregulate not only *Minc16803* but also its orthologous genes. Therefore, it would be interesting to develop RNAi-based transgenic crops to suppress *Minc16803* gene expression in *M. incognita* and even its orthologous genes in other RKNs.

Author contributions

VJVM designed the experiments. VJVM and DHP analyzed the data, and DHP wrote the manuscript. EGJD, PMG, PG, and ACMB searched for nematode gene sequence and analyzed bioinformatics data. MFB performed sequence analysis and produced transgenic *A. thaliana* lines. VJVM performed generation advancements. VJVM, DHP, ITLT, and MELS performed the nematode bioassays. VJVM, ITLT, and JAE performed histological analyses. DHP and ITLT performed RT-qPCR analysis. MFGS, MFB, MCMS, CVM, EGJD, and JAE amended the manuscript. MFGS was the lead researcher, edited the manuscript, and provided financial support and intellectual input. All authors read and approved the final manuscript.

Supplementary Information The online version contains supplementary material available at https://doi.org/10.1007/s10340-023-01623-7.

Acknowledgements The authors acknowledge EMBRAPA, UCB, CNPq, CAPES, INCT PlantStress Biotech, and FAPDF for the scientific and financial support.

Funding This work was supported by grants from INCT PlantStress Biotech, EMBRAPA, CNPq, CAPES, and FAPDF. MFB is grateful to CNPq for a postdoctoral research fellowship (PDJ 150936/2018-4). ITLT is grateful to CAPES/Cofecub project Sv.922/18 for financial support in the researcher and students exchange program between institutions.

Data availability The data that support the findings of this study and any material presented in the manuscript are available from the corresponding author upon reasonable request.

Declarations

Conflict of interest The authors declare no conflict of interest.

References

Ali MA, Azeem F, Li H, Bohlmann H (2017) Smart parasitic nematodes use multifaceted strategies to parasitize plants. Front Plant Sci 8:1–21. https://doi.org/10.3389/fpls.2017.01699

Allen GC, Flores-Vergara MA, Krasynanski S et al (2006) A modified protocol for rapid DNA isolation from plant tissues using cetyltrimethylammonium bromide. Nat Protoc 1:2320–2325. https://doi.org/10.1038/nprot.2006.384

Almagro Armenteros JJ, Tsirigos KD, Sønderby CK et al (2019) SignalP 5.0 improves signal peptide predictions using deep neural networks. Nat Biotechnol 37:420–423. https://doi.org/10.1038/s41587-019-0036-z

Anders S, Pyl PT, Huber W (2015) HTSeq-a python framework to work with high-throughput sequencing data. Bioinformatics 31:166–169. https://doi.org/10.1093/BIOINFORMATICS/BTU638

Basso MF, Lourenço-Tessutti IT, Mendes RAG et al (2020) *MiDaf16-like* and *MiSkn1-like* gene families are reliable targets to develop biotechnological tools for the control and management of *Meloidogyne incognita*. Sci Rep 10:1–13. https://doi.org/10.1038/s41598-020-63968-8

Bauters L, Kyndt T, De Meyer T et al (2020) Chorismate mutase and isochorismatase, two potential effectors of the migratory nematode *Hirschmanniella oryzae*, increase host susceptibility by manipulating secondary metabolite content of rice. Mol Plant Pathol 21:1634–1646. https://doi.org/10.1111/MPP.13003

Bellafiore S, Shen Z, Rosso MN et al (2008) Direct identification of the *Meloidogyne incognita* secretome reveals proteins with host cell reprogramming potential. PLoS Pathog 4:e1000192. https://doi.org/10.1371/JOURNAL.PPAT.1000192

Bernard GC, Egnin M, Bonsi C (2017) The impact of plant-parasitic nematodes on agriculture and methods of control. In: Shah MM, Mahamood M (eds) Nematology–Concepts, Diagnosis and Control. InTech. https://doi.org/10.5772/intechopen.68958

Blanc-Mathieu R, Perfus-Barbeoch L, Aury J-M et al (2017) Hybridization and polyploidy enable genomic plasticity without sex in

the most devastating plant-parasitic nematodes. PLoS Genet 13:e1006777. https://doi.org/10.1371/journal.pgen.1006777
Blum M, Chang HY, Chuguransky S et al (2021) The InterPro protein families and domains database: 20 years on. Nucleic Acids Res 49:D344–D354. https://doi.org/10.1093/NAR/GKAA977
Bybd DW, Kirkpatrick T, Barker KR (1983) An improved technique for clearing and staining plant tissues for detection of nematodes. J Nematol 15:142–143. https://doi.org/10.1079/9781845930561.0059
Canteri MG, Althaus RA, Filho das JSV et al (2001) SASM-AGRI-Sistema para análise e separação de médias em experimentos agrícolas pelos métodos Scott-knott, Tukey e Duncan. Rev Bras Agrocomputação 1:18–24
Castagnone-Sereno P, Danchin EGJ, Perfus-Barbeoch L, Abad P (2013) Diversity and evolution of Root-Knot nematodes, genus Meloidogyne: new insights from the genomic era. Annu Rev Phytopathol 51:203–220. https://doi.org/10.1146/annurev-phyto-082712-102300
Chaudhary S, Dutta TK, Tyagi N et al (2019) Host-induced silencing of *Mi-msp-1* confers resistance to root-knot nematode *Meloidogyne incognita* in eggplant. Transgenic Res 28:327–340. https://doi.org/10.1007/S11248-019-00126-5/FIGURES/6
Chen J, Lin B, Huang Q et al (2017) A novel *Meloidogyne graminicola* effector, MgGPP, is secreted into host cells and undergoes glycosylation in concert with proteolysis to suppress plant defenses and promote parasitism. PLoS Pathog 13:e1006301. https://doi.org/10.1371/journal.ppat.1006301
Chen J, Hu L, Sun L et al (2018) A novel *Meloidogyne graminicola* effector, MgMO237, interacts with multiple host defence-related proteins to manipulate plant basal immunity and promote parasitism. Mol Plant Pathol 19:1942–1955. https://doi.org/10.1111/MPP.12671
Choi I, Subramanian P, Shim D et al (2017) RNA-Seq of plant-parasitic nematode *Meloidogyne incognita* at various stages of its development. Front Genet 8:190. https://doi.org/10.3389/FGENE.2017.00190/BIBTEX
Chu Y, Guimarães LA, Wu CL et al (2014) A technique to study *Meloidogyne arenaria* resistance in *Agrobacterium rhizogenes*-transformed peanut. Research 98:1292–1299. https://doi.org/10.1094/PDIS-12-13-1241-RE
Clough SJ, Bent AF (1998) Floral dip: a simplified method for *Agrobacterium*-mediated transformation of *Arabidopsis thaliana*. Plant J 16:735–743. https://doi.org/10.1046/J.1365-313X.1998.00343.X
Coke MC, Mantelin S, Thorpe P, Lilley CJ, Wright KM, Shaw DS, Chande A, Jones JT, Urwin PE (2021) The GpIA7 effector from the potato cyst nematode *Globodera pallida* targets potato EBP1 and interferes with the plant cell cycle. J Exp Bot 72(20):7301–7315. https://doi.org/10.1093/jxb/erab353
Cunningham F, Allen JE, Allen J et al (2022) Ensembl 2022. Nucleic Acids Res 50:D988–D995. https://doi.org/10.1093/NAR/GKAB1049
Da RM, Bournaud C, Dazenière J et al (2021) Genome expression dynamics reveal the parasitism regulatory landscape of the root-knot nematode *Meloidogyne incognita* and a promoter motif associated with effector genes. Genes (basel) 12:771. https://doi.org/10.3390/GENES12050771
da Silva EH, da Mattos VS, Furlaneto C et al (2014) Genetic variability and virulence of *Meloidogyne incognita* populations from Brazil to resistant cotton genotypes. Eur J Plant Pathol 139:195–204. https://doi.org/10.1007/s10658-014-0381-1
Danchin EGJ, Arguel M-J, Campan-Fournier A et al (2013) Identification of novel target genes for safer and more specific control of root-knot nematodes from a pan-genome mining. PLoS Pathog 9:e1003745. https://doi.org/10.1371/journal.ppat.1003745
Diaz-Granados A, Sterken MG, Overmars H et al (2020) The effector GpRbp-1 of *Globodera pallida* targets a nuclear HECT E3 ubiquitin ligase to modulate gene expression in the host. Mol Plant Pathol 21:66–82. https://doi.org/10.1111/MPP.12880
Dinh PTY, Brown CR, Elling AA (2014) RNA interference of effector gene *Mc16D10L* confers resistance against *Meloidogyne chitwoodi* in *Arabidopsis* and potato. Phytopathology 104:1098–1106. https://doi.org/10.1094/PHYTO-03-14-0063-R
Dutta TK, Papolu PK, Banakar P et al (2015) Tomato transgenic plants expressing hairpin construct of a nematode protease gene conferred enhanced resistance to root-knot nematodes. Front Microbiol 6:260. https://doi.org/10.3389/FMICB.2015.00260
El-Gebali S, Mistry J, Bateman A et al (2019) The Pfam protein families database. Nucleic Acids Res 47:D427–D432. https://doi.org/10.1093/NAR/GKY995
Gardner M, Dhroso A, Johnson N et al (2018) Novel global effector mining from the transcriptome of early life stages of the soybean cyst nematode *Heterodera glycines*. Sci Rep 8:1–15. https://doi.org/10.1038/s41598-018-20536-5
Grynberg P, Togawa RC, de Freitas LD et al (2020) Comparative genomics reveals novel target genes towards specific control of plant-parasitic nematodes. Genes (basel) 11:1–25. https://doi.org/10.3390/genes11111347
Habash SS, Radakovic ZS, Vankova R et al (2017) *Heterodera schachtii* tyrosinase-like protein—a novel nematode effector modulating plant hormone homeostasis. Sci Rep 7:1–10. https://doi.org/10.1038/s41598-017-07269-7
Howe KL, Bolt BJ, Shafie M et al (2017) WormBase ParaSite – a comprehensive resource for helminth genomics. Mol Biochem Parasitol 215:2. https://doi.org/10.1016/J.MOLBIOPARA.2016.11.005
Hu Y, You J, Li C et al (2019) The *Heterodera glycines* effector Hg16B09 is required for nematode parasitism and suppresses plant defense response. Plant Sci 289:110271. https://doi.org/10.1016/J.PLANTSCI.2019.110271
Huang G, Allen R, Davis EL et al (2006) Engineering broad root-knot resistance in transgenic plants by RNAi silencing of a conserved and essential root-knot nematode parasitism gene. Proc Natl Acad Sci U S A 103:14302–14306. https://doi.org/10.1073/pnas.0604698103
Jagdale S, Rao U, Giri AP (2021) Effectors of root-knot nematodes: an arsenal for successful parasitism. Front Plant Sci 12:800030. https://doi.org/10.3389/FPLS.2021.800030
Joshi I, Kumar A, Singh AK et al (2019) Development of nematode resistance in arabidopsis by HD-RNAi-mediated silencing of the effector gene Mi-msp2. Sci Rep 9:17404. https://doi.org/10.1038/s41598-019-53485-8
Joshi I, Kumar A, Kohli D et al (2020) Conferring root-knot nematode resistance via host-delivered RNAi-mediated silencing of four *Mi-msp* genes in *Arabidopsis*. Plant Sci 298:110592. https://doi.org/10.1016/j.plantsci.2020.110592
Kim D, Pertea G, Trapnell C et al (2013) TopHat2: accurate alignment of transcriptomes in the presence of insertions, deletions and gene fusions. Genome Biol 14:1–13. https://doi.org/10.1186/GB-2013-14-4-R36/FIGURES/6
Koenning SR, Barker KR, Bowman DT (2001) Resistance as a tactic for management of *Meloidogyne incognita* on cotton in North Carolina. J Nematol 33:126
Kyndt T, Vieira P, Gheysen G, de Almeida-Engler J (2013) Nematode feeding sites: unique organs in plant roots. Planta 238:807–818. https://doi.org/10.1007/s00425-013-1923-z
Lee RYN, Howe KL, Harris TW et al (2018) WormBase 2017: molting into a new stage. Nucleic Acids Res 46:D869–D874. https://doi.org/10.1093/NAR/GKX998
Leelarasamee N, Zhang L, Gleason C (2018) The root-knot nematode effector MiPFN3 disrupts plant actin filaments and promotes parasitism. PLoS Pathog 14:e1006947. https://doi.org/10.1371/journal.ppat.1006947

Lin B, Zhuo K, Chen S et al (2016) A novel nematode effector suppresses plant immunity by activating host reactive oxygen species-scavenging system. New Phytol 209:1159–1173. https://doi.org/10.1111/nph.13701

Lisei-de-Sá ME, Rodrigues-Silva PL, Morgante CV et al (2021) Pyramiding dsRNAs increases phytonematode tolerance in cotton plants. Planta 254:254–121. https://doi.org/10.1007/S00425-021-03776-0

Lourenço-Tessutti IT, Souza JDA, Martins-de-Sa D et al (2015) Knock-down of heat-shock protein 90 and isocitrate lyase gene expression reduced root-knot nematode reproduction. Phytopathology 105:628–637. https://doi.org/10.1094/PHYTO-09-14-0237-R

Lück S, Kreszies T, Strickert M et al (2019) siRNA-Finder (si-Fi) software for RNAi-target design and off-target prediction. Front Plant Sci 10:1023. https://doi.org/10.3389/fpls.2019.01023

Marchler-Bauer A, Derbyshire MK, Gonzales NR et al (2015) CDD: NCBI's conserved domain database. Nucleic Acids Res 43:D222–D226. https://doi.org/10.1093/NAR/GKU1221

Mejias J, Truong NM, Abad P et al (2019) Plant proteins and processes targeted by parasitic nematode effectors. Front Plant Sci 10:970. https://doi.org/10.3389/fpls.2019.00970

Mejias J, Bazin J, Truong NM et al (2021) The root-knot nematode effector MiEFF18 interacts with the plant core spliceosomal protein SmD1 required for giant cell formation. New Phytol 229:3408–3423. https://doi.org/10.1111/nph.17089

Mendes RAG, Basso MF, Fernandes J et al (2021a) Minc00344 and Mj-NULG1a effectors interact with GmHub10 protein to promote the soybean parasitism by *Meloidogyne incognita* and *M. javanica*. Exp Parasitol 229:108153. https://doi.org/10.1016/j.exppara.2021.108153

Mendes RAG, Basso MF, Paes-de-Melo B et al (2021b) The Mi-EFF1/Minc17998 effector interacts with the soybean GmHub6 protein to promote host plant parasitism by *Meloidogyne incognita*. Physiol Mol Plant Pathol 114:1–11. https://doi.org/10.1016/j.pmpp.2021.101630

Möller S, Croning MDR, Apweiler R (2001) Evaluation of methods for the prediction of membrane spanning regions. Bioinformatics 17:646–653. https://doi.org/10.1093/BIOINFORMATICS/17.7.646

Moreira VJV, Lourenço-Tessutti IT, Basso MF et al (2022) *Minc03328* effector gene downregulation severely affects *Meloidogyne incognita* parasitism in transgenic *Arabidopsis thaliana*. Planta 255:1–16. https://doi.org/10.1007/S00425-022-03823-4

Murashige T, Skoog F (1962) A revised medium for rapid growth and bio assays with tobacco tissue cultures. Physiol Plant 15:473–497. https://doi.org/10.1111/j.1399-3054.1962.tb08052.x

Nguyen Ba AN, Pogoutse A, Provart N, Moses AM (2009) NLStradamus: a simple hidden markov model for nuclear localization signal prediction. BMC Bioinform 10:1–11. https://doi.org/10.1186/1471-2105-10-202/FIGURES/7

Niu J, Liu P, Liu Q et al (2016) Msp40 effector of root-knot nematode manipulates plant immunity to facilitate parasitism. Sci Rep 6:1–13. https://doi.org/10.1038/srep19443

Oka Y (2020) From old-generation to next-generation nematicides. Agronomy 10:1387. https://doi.org/10.3390/agronomy10091387

Orfanoudaki G, Markaki M, Chatzi K et al (2017) MatureP: prediction of secreted proteins with exclusive information from their mature regions. Sci Rep 7:3263. https://doi.org/10.1038/s41598-017-03557-4

Pak J, Fire A (2007) Distinct populations of primary and secondary effectors during RNAi in *C. elegans*. Science 315(5809):241–244. https://doi.org/10.1126/science.1132839

Pfaffl MW (2001) A new mathematical model for relative quantification in real-time RT-PCR. Nucleic Acids Res 29:e45. https://doi.org/10.1093/nar/29.9.e45

Pogorelko G, Juvale PS, Rutter WB et al (2016) A cyst nematode effector binds to diverse plant proteins, increases nematode susceptibility and affects root morphology. Mol Plant Pathol 17:832–844. https://doi.org/10.1111/MPP.12330

Pogorelko G, Wang J, Juvale PS et al (2020) Screening soybean cyst nematode effectors for their ability to suppress plant immunity. Mol Plant Pathol 21:1240–1247. https://doi.org/10.1111/MPP.12972

Qin X, Xue B, Tian H et al (2021) An unconventionally secreted effector from the root knot nematode *Meloidogyne incognita*, Mi-ISC-1, promotes parasitism by disrupting salicylic acid biosynthesis in host plants. Mol Plant Pathol 00:1–14. https://doi.org/10.1111/MPP.13175

Rutter WB, Hewezi T, Abubucker S et al (2014) Mining novel effector proteins from the eMining novel effector proteins from the esophageal gland cells of *Meloidogyne incognita*. Mol Plant-Microbe Interact 27:965–974. https://doi.org/10.1094/MPMI-03-14-0076-R

Siddique S, Grundler FM (2018) Parasitic nematodes manipulate plant development to establish feeding sites. Curr Opin Microbiol 46:102–108. https://doi.org/10.1016/j.mib.2018.09.004

Sindhu AS, Maier TR, Mitchum MG et al (2009) Effective and specific *in planta* RNAi in cyst nematodes: expression interference of four parasitism genes reduces parasitic success. J Exp Bot 60:315–324. https://doi.org/10.1093/jxb/ern289

Smith NA, Singh SP, Wang MB et al (2000) Total silencing by intronspliced hairpin RNAs. Nature 407:319–320. https://doi.org/10.1038/35030305

Song H, Lin B, Huang Q et al (2021) The *Meloidogyne javanica* effector Mj2G02 interferes with jasmonic acid signalling to suppress cell death and promote parasitism in *Arabidopsis*. Mol Plant Pathol 22:1288–1301. https://doi.org/10.1111/MPP.13111

Souza Júnior JDA, Coelho RR, Lourenço IT et al (2013) Knocking-down *Meloidogyne incognita* proteases by plant-delivered dsRNA has negative pleiotropic effect on nematode vigor. PLoS ONE 8:85364. https://doi.org/10.1371/journal.pone.0085364

Steeves RM, Todd TC, Essig JS, Trick HN (2006) Transgenic soybeans expressing siRNAs specific to a major sperm protein gene suppress *Heterodera glycines* reproduction. Funct Plant Biol 33:991–999. https://doi.org/10.1071/FP06130

Taylor AL, Sasser JN (1978) Biology, identification and control of root-knot nematodes. North Carolina State University Graphics, 111

Tian B, Li J, Vodkin LO et al (2019) Host-derived gene silencing of parasite fitness genes improves resistance to soybean cyst nematodes in stable transgenic soybean. Theor Appl Genet 132:2651–2662. https://doi.org/10.1007/S00122-019-03379-0/FIGURES/7

Triantaphyllou AC, Hirschmann H (1960) Post infection development of *Meloidogyne incognita* chitwood 1949 (nematoda-heteroderidae). Ann L'institut Phytopathol Benaki 3:1–11

Truong NM, Chen Y, Mejias J et al (2021) The *Meloidogyne incognita* nuclear effector MiEFF1 interacts with *Arabidopsis* cytosolic glyceraldehyde-3-phosphate dehydrogenases to promote parasitism. Front Plant Sci 12:641480. https://doi.org/10.3389/fpls.2021.641480

Vandesompele J, De Preter K, Pattyn F et al (2002) Accurate normalization of real-time quantitative RT-PCR data by geometric averaging of multiple internal control genes. Genome Biol 3(7):research0034.1. https://doi.org/10.1186/gb-2002-3-7-research0034

Vens C, Rosso MN, Danchin EGJ (2011) Identifying discriminative classification-based motifs in biological sequences. Bioinformatics 27:1231–1238. https://doi.org/10.1093/BIOINFORMATICS/BTR110

Verma A, Lee C, Morriss S et al (2018) The novel cyst nematode effector protein 30D08 targets host nuclear functions to alter gene

expression in feeding sites. New Phytol 219:697–713. https://doi.org/10.1111/NPH.15179
Vieira P, Gleason C (2019) Plant-parasitic nematode effectors — insights into their diversity and new tools for their identification. Curr Opin Plant Biol 50:37–43. https://doi.org/10.1016/j.pbi.2019.02.007
Wang J, Lee C, Replogle A et al (2010) Dual roles for the variable domain in protein trafficking and host-specific recognition of *Heterodera glycines* CLE effector proteins. New Phytol 187:1003–1017. https://doi.org/10.1111/j.1469-8137.2010.03300.x
Wheeler TA, Siders KT, Anderson MG et al (2014) Management of *Meloidogyne incognita* with chemicals and cultivars in cotton in a semi-arid environment. J Nematol 46:101
Xie J, Li S, Mo C et al (2016) A novel *Meloidogyne incognita* effector Misp12 suppresses plant defense response at latter stages of nematode parasitism. Front Plant Sci 7:964. https://doi.org/10.3389/fpls.2016.00964
Zhang J, Coaker G, Zhou JM, Dong X (2020) Plant immune mechanisms: from reductionistic to holistic points of view. Mol Plant 13:1358–1378. https://doi.org/10.1016/J.MOLP.2020.09.007
Zhao J, Li L, Liu Q et al (2019) A MIF-like effector suppresses plant immunity and facilitates nematode parasitism by interacting with plant annexins. J Exp Bot 70:5943–5958. https://doi.org/10.1093/jxb/erz348
Zhao J, Mejias J, Quentin M et al (2020) The root-knot nematode effector MiPDI1 targets a stress-associated protein (SAP) to establish disease in Solanaceae and *Arabidopsis*. New Phytol 228:1417–1430. https://doi.org/10.1111/nph.16745
Zhou E, Wheeler TA, Starr JL (2000) Root galling and reproduction of *Meloidogyne incognita* isolates from Texas on resistant cotton genotypes. J Nematol 32:513–518
Zhuo K, Chen J, Lin B et al (2017) A novel *Meloidogyne enterolobii* effector MeTCTP promotes parasitism by suppressing programmed cell death in host plants. Mol Plant Pathol 18:45–54. https://doi.org/10.1111/MPP.12374
Zhuo K, Naalden D, Nowak S et al (2019) A *Meloidogyne graminicola* C-type lectin, Mg01965, is secreted into the host apoplast to suppress plant defence and promote parasitism. Mol Plant Pathol 20:346–355. https://doi.org/10.1111/MPP.12759